THE SECOND-ORDER ABERRATIONS

As an application of the foregoing theory we calculate the ion orbits up to the second order in an apparatus with two successive fields with an intermediate image, the usual configuration in most mass spectrographs. The descriptive quantities of the fields, W, α, γ, p, q, r, etc. are indexed I and II. The lateral radial magnifications are given in Eq. (13). The index n taking the values 1, 2, 3, and 4 are used to denote the object space of the first field, the image space of I, the object space of II, and the image space of II, respectively. So, $p_1=p_{\mathrm{I}}'$, $p_2=p_{\mathrm{I}}''$, $p_3=p_{\mathrm{II}}'$, and $p_4=p_{\mathrm{II}}''$; $\alpha_1=\alpha_2=\alpha_{\mathrm{I}}$, $\alpha_3=\alpha_4=\alpha_{\mathrm{II}}$, etc. The actual value of the radial magnification is given by M_n, so $M_1=1$, $M_2=M_{\mathrm{lat\ I}}=M_3$, $M_4=M_{\mathrm{lat\ I}}\cdot M_{\mathrm{lat\ II}}$. The final expression for y_{II}'' now becomes

$$y_{\mathrm{II}}''=\sum_n M_{5-n}(P_n+Q_n\cos A_n+R_n\sin A_n+S_n\cos 2A_n+T_n\sin 2A_n+U_n\cos 2\Gamma_n+V_n\sin 2\Gamma_n).$$

This is still the general expression for y_{II}''. To find the aberrations, conditions like Eq. (24) or Eq. (25) have to be introduced to make the variable first-order terms equal to zero, as shown in Part I. This conditional general expression contains the essential possibilities to correct for the second-order aberrations.

ACKNOWLEDGMENTS

The author wishes to express his gratitude to Professor Dr. J. Kistemaker for his stimulating interest in these calculations. This work is part of the research program of the "Stichting voor Fundamenteel Onderzoek der Materie" and was made possible by financial support from the "Nederlandse Organisatie voor Zuiver Wetenschappelijk Onderzoek."

JOURNAL OF APPLIED PHYSICS VOLUME 35, NUMBER 6 JUNE 1964

Theory of Current Collection of Moving Cylindrical Probes

MADHOO KANAL
Space Physics Research Laboratory, The University of Michigan, Ann Arbor, Michigan
(Received 7 October 1963)

The theory of current collection of a moving cylindrical probe is investigated. Volt–ampere relations are derived for two distinct cases: (i) The general-ion current for accelerating collector potential and its special cases, including general-ion current to the stationary probe, orbital-motion-limited current to the moving and the stationary probes, and sheath-area-limited current to the moving and the stationary probes; (ii) the general-electron current for the retarding collector potential and its special cases, including general-electron current to the stationary probe and random-electron current to the moving and the stationary probes. Orientation of the cylinder with respect to the drift velocity vector is taken into account. Volt–ampere characteristics are included for illustrating the functional behavior of the current relations.

I. INTRODUCTION

IN recent years, with the advent of multi-experimental satellites, single cylindrical collectors have gained considerable popularity. In all these experiments, as is normal even for rocket-borne probes, the probe velocity exceeds the thermal velocity of the ions for much of the flight. The data, consequently, indicate strong effects of the probe motion on the ion current collected by the device, thereby drawing attention to the need for a theoretical development which would permit the volt–ampere relation to be predicted as a function of the probe velocity.

In 1926 Mott-Smith and Langmuir[1,2] published their classic paper on probe theory, in which they derived the volt–ampere relations for spherical, cylindrical, and planar probe geometries. However, their theory was limited to a stationary plasma except in the case of the cylindrical probe having a diameter many orders of magnitude smaller than the diameter of the ion sheath surrounding the collector. In this paper the problem of a moving cylindrical probe with a nonvanishing collector-to-ion-sheath-diameter ratio is treated. Two cases of current collection are considered depending on whether the probe potential is accelerating or retarding the particles under consideration. From these two general relations some specific cases of special interest are deduced and discussed. The problem of the moving spherical probe has been treated elsewhere.[3–6]

[1] H. M. Mott-Smith and I. Langmuir, Phys. Rev. **28**, 727 (1926).
[2] I. Langmuir, Rev. Mod. Phys. **3**, 191 (1931).
[3] G. Medicus, J. Appl. Phys. **32**, 2512 (1961).
[4] M. Kanal, "Theory of Current Collection of Moving Spherical Probes," University of Michigan, ORA Report No. 03599-9-S, Ann Arbor (1962); (unpublished).
[5] R. C. Sagalyn, M. Smiddy, and J. Wisvia, J. Geophys. Res. **68**, 199 (1963).
[6] A. F. Nagy, L. H. Brace, G. R. Carignan, and M. Kanal, J. Geophys. Res. **68**, 6401 (1963).

General Considerations

When a conducting electrode is immersed in a plasma consisting of positive ions and electrons in thermal equilibrium, the resulting collisions of the charged particles with the electrode cause it to assume a potential with respect to the plasma such that the net current to the collector is zero. The magnitude of this equilibrium potential is mainly determined by the square root of the ion-to-electron mass ratio, and the polarity of the collector is negative. The collector potential causes a region of positive charge to build up about the probe in which the electrons are repelled and the positive ions are attracted. Such a region is commonly called a positive-ion sheath. The boundary of the sheath is defined as that distance beyond which the charged particles experience negligible force due to the collector potential.

In order to study the current collection characteristics of a moving cylindrical probe, some assumption in regard to the sheath configuration is necessary. Although the cylindrical shape of the sheath is not maintained at high probe velocities, no sufficiently precise model is available which will justify empirically or theoretically any other shape. Therefore, as a first-order approximation, a cylindrical sheath is assumed.

In this work the classical definition of the sheath is used, i.e., the effect of the "presheath" is neglected. The magnitude of the error introduced by this simplifying assumption, as shown by Schultz and Brown,[7] is small. However, recent work by Medicus (private communication) indicates that the error under certain conditions may be significant. In the ionosphere the ratio T_e/T_i is usually between one and two, and Medicus agrees with the conclusions of Schultz and Brown that the significance of the "presheath" decreases as T_e/T_i approaches unity.

Finally, it is assumed that the velocity distribution of the particles in the undisturbed plasma is Maxwellian. With respect to the moving probe this distribution appears to be superimposed on the drift velocity of the vehicle.

II. THEORY

1. Superimposed Maxwellian Distribution

Consider an oblique view of the cylindrical sheath shown in Fig. 1. Let u_x', u_y', u_z', be the particle velocity components in the space-fixed coordinate system x', y', z'. Further let u_x, u_y, u_z be the particle velocity components in a coordinate system x, y, z fixed on the moving probe and parallel to the primed system. Choose the y axis along the axis of the cylinder, as shown. If W is the probe velocity and θ the angle between the **W** vector and the y axis, then the transformation equations between the velocity components in the two-coordinate

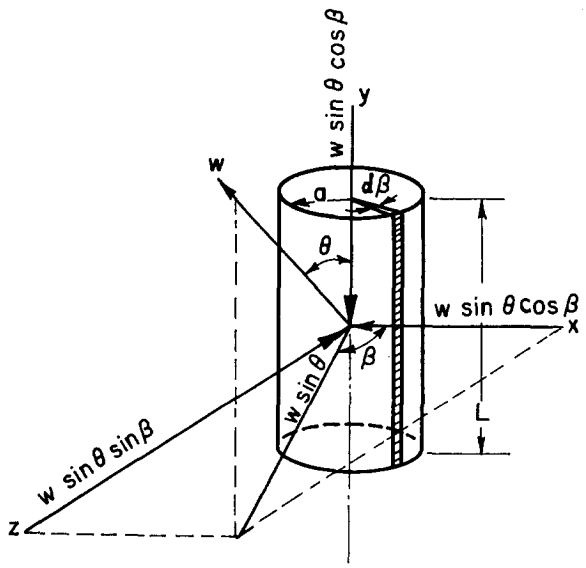

FIG. 1. Velocity space coordinates at the sheath edge.

systems are

$$\begin{aligned} u_x &= u_x' + W\sin\theta\cos\beta, \\ u_y &= u_y' + W\cos\theta, \\ u_z &= u_z' + W\sin\theta\sin\beta, \end{aligned} \tag{1}$$

where β is the azimuth angle of **W** with respect to the x axis.

Let N be the number density of one kind of particles in the plasma, T the temperature, and m their mass; then the Maxwellian velocity distribution of the particles with respect to the stationary coordinate system is,

$$f(u_x',u_y',u_z')du_x'du_y'du_z' = [N/(\pi C_m^2)^{\frac{3}{2}}] \times \exp[-(1/C_m^2)(u_x'^2+u_y'^2+u_z'^2)]du_x'du_y'du_z', \tag{2}$$

where C_m is the most probably velocity of the particles defined as $C_m = (2kT/m)^{\frac{1}{2}}$, k being Boltzmann's constant.

With respect to the moving system the distribution function (2) is modified in a way determined by the linear transformations of the velocity components given in (1). Thus for the moving system the new distribution function at the sheath edge is

$$\begin{aligned} &F(u_x,u_y,u_z,\beta)du_xdu_ydu_z \\ &= [N/(\pi C_m^2)^{\frac{3}{2}}]\exp\{-(1/C_m^2)[(u_x - W\sin\theta\cos\beta)^2 \\ &+ (u_y - W\cos\theta)^2 + (u_z - W\sin\theta\sin\beta)^2]\}du_xdu_ydu_z. \end{aligned} \tag{3}$$

2. Development of the Current Equations

In Fig. 1 consider an infinitesimal strip of area $La d\beta$ on the sheath surface normal to the x axis, where a is the sheath radius. The number of particles with velocity ranges between u_x and u_x+du_x, u_y and u_y+du_y and u_z and u_z+du_z that are expected to cross the infinitesimal area per unit time is given by

$$La u_x F(u_x,u_y,u_z)du_xdu_ydu_zd\beta, \tag{4}$$

where L is the length of the cylinder.

[7] G. J. Schulz and S. C. Brown, Phys. Rev. **98**, 1642 (1955).

On multiplying (4) with the electronic charge and integrating between proper limits the following equation for the current collected by the moving probe is obtained.

$$I=Lae\int_{\beta=0}^{2\pi}\int_{u_x=0,\,u_1}^{\infty}\int_{u_z=-\infty}^{\infty}\int_{u_z=-p}^{p} u_x F(u_x,u_y,u_x,\beta) \times du_x du_y du_z d\beta. \quad (5)$$

The lower limit of u_x in (5) is zero when the collector potential attracts the charged particles entering the sheath and it is $u_1=(2eV/m)^{\frac{1}{2}}$ when it repels them, V being the collector potential. The former type of the collected current is referred to as the "accelerated current" and the latter as the "retarded current." The limits of u_y from $-\infty$ to ∞ follow from the assumption that $L\gg r$, where r is the collector radius. If in a plane normal to the cylinder axis u_x is the radial component at the sheath surface, then u_z represents the tangential component. By applying the laws of conservation of energy and angular momentum to the charged-particle trajectory in the sheath one obtains the following equation for the value of $u_z=p$ necessary for the collection of the particle:

$$p^2=\gamma_0^2(u_x^2+2eV/m), \quad (6)$$

where $\gamma_0^2=r^2/(a^2-r^2)$. In (6) $V>0$ for the accelerating collector potential and $V<0$ for the retarding case.

It is easy to integrate (5) with respect to β and u_y. The result is

$$I=\frac{4LNae}{C_m^2}e^{-\kappa^2}\int_{0,\,u_1}^{\infty}\int_{0}^{p} u_x \exp\left\{-\left[\frac{u_x^2+u_z^2}{C_m^2}\right]\right\} \times I_0\left(\frac{2\kappa}{C_m}(u_x^2+u_z^2)^{\frac{1}{2}}\right)du_x du_z, \quad (7)$$

where $I_0(x)$ is the modified Bessel function of the zero order and $\kappa=(W/C_m)\sin\theta$.

It is seen that Eq. (6) describes a hyperbola whose vertices are $(\gamma_0(2eV/m)^{\frac{1}{2}},0)$ for $V>0$ on the p axis and $(0,(2eV/m)^{\frac{1}{2}})$ for $V<0$ on the u_x axis, as shown in Figs. 2 and 3, respectively.

Since the integrand of (7) is an even function of u_z, it is sufficient to show only one branch of each hyperbola and the limit of u_z is then taken from 0 to p.

For the purpose of integrating (7) it is convenient to introduce the polar coordinates as given below:

$$u_x/C_m=s\cos\phi,\quad u_z/C_m=s\sin\phi,\quad du_z du_z=C_m^2 s\,ds\,d\phi. \quad (8)$$

Divide both sides of Eq. (6) by C_m^2 and let $2eV/mC_m^2=eV/kT=V_0$ to obtain

$$p^2/C_m^2=\gamma_0^2(u_x^2/C_m^2+V_0). \quad (9)$$

In order to obtain the new limits of integration, substitute Eq. (8) into Eq. (9) (for $u_z=p$) and solve for ϕ. Thus,

$$\phi_1=\sin^{-1}[\gamma_0^2(s^2+V_0)/s^2(1+\gamma_0^2)]^{\frac{1}{2}}, \quad (10)$$

where ϕ_1 is the upper limit of ϕ.

Now the two cases $V_0>0$ and $V_0<0$ will be considered separately, using the above transformations, and the corresponding volt-ampere relations derived.

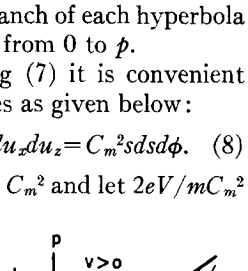

FIG. 2. Hyperbola generated in velocity space coordinate system by p as a function of u_x, when the collector potential is accelerating.

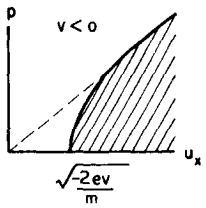

FIG. 3. Hyperbola generated in velocity space coordinate system by p as a function of u_x when the collector potential is retarding.

3. Accelerated Current ($V_0>0$)

From Fig. 2 it is clear that for $V_0>0$ the domain of integration is

$$0\le\phi\le\tfrac{1}{2}\pi,\quad 0\le s\le\gamma_0 V_0^{\frac{1}{2}}, \quad (11a)$$

and

$$0\le\phi\le\phi_1,\quad \gamma_0 V_0^{\frac{1}{2}}\le s<\infty, \quad (11b)$$

where ϕ_1 is given by (10).

Insertion of (8) in (7) using the limits given in (11a) and (11b) and integrating with respect to ϕ leads to the following single integral for the accelerated current (I_a):

$$I_a=\left(\frac{kT}{2m\pi}\right)^{\frac{1}{2}}NeA_c\frac{4}{\pi^{\frac{1}{2}}}e^{-\kappa^2}\left[\int_{\gamma_0 V_0^{\frac{1}{2}}}^{\infty} s(s^2+V_0)^{\frac{1}{2}}e^{-s^2}I_0(2\kappa s)ds + \left(\frac{1+\gamma_0^2}{\gamma_0^2}\right)^{\frac{1}{2}}\int_0^{\gamma_0 V_0^{\frac{1}{2}}} s^2 e^{-s^2}I_0(2\kappa s)ds\right], \quad (12)$$

where $A_c=2\pi rL$, the surface area of the collector, and C_m in (7) is replaced by $(2kT/m)^{\frac{1}{2}}$.

In order to help in visualizing the effect of the sheath and the probe motion upon the current collection, the current equations are normalized with respect to a quantity called the "random current," I_d. This random current is defined as the current resulting from the random motion of one kind of particle when the sheath thickness and the vehicle velocity are zero ($a=r$, $W=0$). If one sets $\kappa=0$ and $\gamma_0=[r^2/(a^2-r^2)]^{\frac{1}{2}}=\infty$, in (12), then

$$I_d=(kT/2m\pi)^{\frac{1}{2}}NeA_c, \quad (13)$$

which is the product of the current density and the collector area. Now we define the normalized current I_{an} as

$$I_{an}=I_a/I_d, \quad (14)$$

where I_a is given by (12). Equation (12) in the form of

(14) then becomes

$$I_{an}=\frac{4}{\pi^{\frac{1}{2}}}e^{-\kappa^2}\left[\int_{\gamma_0V_0^{\frac{1}{2}}}^{\infty}s(s^2+V_0)^{\frac{1}{2}}e^{-s^2}I_0(2\kappa s)ds+\left(\frac{1+\gamma_0^2}{\gamma_0^2}\right)^{\frac{1}{2}}\int_0^{\gamma_0V_0^{\frac{1}{2}}}s^2e^{-s^2}I_0(2\kappa s)ds\right]. \quad (15)$$

To solve (15) take its first integral and let $s^2+V_0=t$. Then write

$$\begin{aligned}I_1&=\int_{\gamma_0V_0^{\frac{1}{2}}}^{\infty}s(s^2+V_0)^{\frac{1}{2}}e^{-s^2}I_0(2\kappa s)ds\\&=\tfrac{1}{2}e^{V_0}\int_{V_0(1+\gamma_0^2)}^{\infty}t^{\frac{1}{2}}e^{-t}I_0(2\kappa(t-V_0)^{\frac{1}{2}})dt\\&=\tfrac{1}{2}e^{V_0}\sum_{k=0}^{\infty}\sum_{n=0}^{k}\frac{\kappa^{2k}(-V_0)^{k-n}}{k!(k-n)!n!}\int_{V_0(1+\gamma_0^2)}^{\infty}t^{n+\frac{1}{2}}e^{-t}dt,\\I_1&=\tfrac{1}{2}e^{V_0}\sum_{k=0}^{\infty}\sum_{n=0}^{k}\frac{\kappa^{2k}(-V_0)^{k-n}}{k!(k-n)!n!}\Gamma(n+\tfrac{3}{2},V_0(1+\gamma_0^2)),\end{aligned} \quad (16)$$

where $\Gamma(n+\frac{3}{2}, V_0(1+\gamma_0^2))$ is the incomplete gamma function defined as

$$\Gamma(\nu,\chi)=\int_{\chi}^{\infty}e^{-t}t^{\nu-1}dt.$$

Upon using the following Lemma[8] in (16)

$$\sum_{k=0}^{\infty}\sum_{n=0}^{k}A(k,n)=\sum_{k,n=0}^{\infty}A(k+n,n),$$

one obtains

$$\begin{aligned}I_1&=\tfrac{1}{2}e^{V_0}\sum_{n,k=0}^{\infty}\frac{\kappa^{2k+2n}(-V_0)^k}{(k+n)!k!n!}\Gamma(n+\tfrac{3}{2},V_0(1+\gamma_0^2)),\\I_1&=\tfrac{1}{2}e^{V_0}\sum_{n=0}^{\infty}\frac{\kappa^n}{n!V_0^{n/2}}\Gamma(n+\tfrac{3}{2},V_0(1+\gamma_0^2))J_n(2\kappa V_0^{\frac{1}{2}}).\end{aligned} \quad (17)$$

The second integral of (15) is similarly solved by expanding the modified Bessel function in its power-series form. Thus

$$\begin{aligned}I_2&=\int_0^{\gamma_0V_0^{\frac{1}{2}}}s^2e^{-s^2}I_0(2\kappa s)ds\\&=\sum_{n=0}^{\infty}\frac{\kappa^{2n}}{(n!)^2}\int_0^{\gamma_0V_0^{\frac{1}{2}}}s^{2n+2}e^{-s^2}ds,\\I_2&=\tfrac{1}{2}\sum_{n=0}^{\infty}\frac{\kappa^{2n}}{(n!)^2}\gamma(n+\tfrac{3}{2},\gamma_0^2V_0),\end{aligned} \quad (18)$$

where $\gamma(n+\frac{3}{2}, \gamma_0^2V_0)$ is also an incomplete gamma function, however, defined as

$$\gamma(\nu,\chi)=\int_0^{\chi}e^{-t}t^{\nu-1}dt.$$

Substitute (17) and (18) into (15) to get

$$I_{an}=\frac{2}{\pi^{\frac{1}{2}}}e^{-\kappa^2}\sum_{n=0}^{\infty}\frac{\kappa^n}{n!}\left[e^{V_0}V_0^{-n/2}\Gamma(n+\tfrac{3}{2},V_0(1+\gamma_0^2))\times J_n(2\kappa V_0^{\frac{1}{2}})+\frac{a}{r}\frac{\kappa^n}{n!}\gamma(n+\tfrac{3}{2},\gamma_0^2V_0)\right]. \quad (19)$$

Equation (19) represents the normalized "accelerated current" volt–ampere relation as a function of the probe velocity and its orientation when the sheath thickness about the collector is finite.

The stationary probe characteristic relation may be deduced from (19) by letting $\kappa=0$. The result is

$$I_{an}|_{\kappa=0}=\frac{2}{\pi^{\frac{1}{2}}}\left[e^{V_0}\Gamma(\tfrac{3}{2},V_0(1+\gamma_0^2))+\frac{a}{r}\gamma(\tfrac{3}{2},\gamma_0^2V_0)\right]. \quad (20)$$

In accordance with the definitions of the incomplete gamma functions Eq. (20) may be rewritten as

$$I_{an}|_{\kappa=0}=e^{V_0}\operatorname{erfc}(V_0^{\frac{1}{2}}(1+\gamma_0^2)^{\frac{1}{2}})+\frac{a}{r}\operatorname{erf}(\gamma_0V_0^{\frac{1}{2}}), \quad (21)$$

where

$$\operatorname{erf}(\chi)=\frac{2}{\pi^{\frac{1}{2}}}\int_0^{\chi}e^{-t^2}dt$$

is the probability integral and $\operatorname{erfc}(\chi)$ is the complimentary error function defined as $1-\operatorname{erf}(\chi)$.

Other special cases of interest are the two asymptotic solutions of (12) which are obtained by letting $a/r\to 1$ $(\gamma_0\to\infty)$ and $a/r\to\infty$ $(\gamma_0\to 0)$. The former solution is referred to as "sheath-area limited" and the latter as "orbital-motion limited." In the first case $(a/r\to 1)$ all the particles that enter the sheath are collected. Consequently, the totality of the accelerated current to the probe is limited only by the area of the sheath. In the second case $(a/r\to\infty)$ the accelerated current to the probe is independent of a/r and depends only upon the net voltage across the sheath.

The equation for the sheath-area-limited current I_s (first asymptotic solution) may either be derived from (12) or simply deduced from Eq. (19) by letting $a/r\to 1(\gamma_0\to\infty)$. In either case the result in the normalized form, $I_{sn}=I_s/I_d$ is given below:

$$I_{sn}=(a/r)e^{-\kappa^2}[(1+\kappa^2)I_0(\tfrac{1}{2}\kappa^2)+\kappa^2I_1(\tfrac{1}{2}\kappa^2)]. \quad (22)$$

For $\kappa=0$, meaning either $W=0$ or $\theta=0$, Eq. (22) reduces to

$$I_{sn}|_{\kappa=0}=a/r. \quad (23)$$

[8] E. D. Rainville, *Special Functions* (The Macmillan Company, New York, 1960).

When Eq. (22) is multiplied by I_d given in (13) one sees that r in the denominator is canceled, and I_s is equal to the product of the current density and the area of the sheath, as expected.

The equation for the orbital-motion-limited current I_0 (second asymptotic solution) may directly be obtained from (19) by letting $a/r \to \infty$ ($\gamma_0 \to 0$). The result in the normalized form $I_{0n}=I_0/I_d$ is, then, given by

$$I_{0n}=\frac{2}{\pi^{\frac{1}{2}}}e^{V_0-\kappa^2}\sum_{n=0}^{\infty}\frac{\kappa^n}{n!V_0{}^{n/2}}\Gamma(n+\tfrac{3}{2},V_0)J_n(2\kappa V_0{}^{\frac{1}{2}}). \quad (24)$$

For $\kappa=0$, Eq. (24) reduces to

$$I_{0n}|_{\kappa=0}=\frac{2}{\pi^{\frac{1}{2}}}V_0{}^{\frac{1}{2}}+e^{V_0}\operatorname{erfc}(V_0{}^{\frac{1}{2}}). \quad (25)$$

For values of $V_0 \geq 5$, Eq. (25) can be approximated by

$$I_{0n}|_{\kappa=0}\cong\frac{2}{\pi^{\frac{1}{2}}}(1+V_0)^{\frac{1}{2}}. \quad (26)$$

Equation (25) and its approximation given in (26) are well known and have been used extensively in laboratory plasma studies.[1,2] In the study of the ionosphere, however, by means of probes carried by sounding rockets or satellites, the probe motion makes it imperative to use the velocity containing equations discussed above.

4. Retarded Current ($V_0<0$)

When a particle enters the sheath and experiences a repulsive field ($V_0<0$), the least radial velocity component required for its collection is $(2eV_0/m)^{\frac{1}{2}}$. From Fig. 3, which is a plot of Eq. (6) for $V_0<0$, the domain of integration for Eq. (7) in polar coordinates is,

$$0\leq\phi\leq\phi_1, \quad V_0{}^{\frac{1}{2}}\leq s<\infty.$$

The resulting single integral for the retarded current I_r is then

$$I_r=\left(\frac{kT}{2m\pi}\right)^{\frac{1}{2}}NeA_c\frac{4}{\pi^{\frac{1}{2}}}e^{-\kappa^2}\int_{(-V_0)^{\frac{1}{2}}}^{\infty}s(s^2+V_0)^{\frac{1}{2}}e^{-s^2}I_0(2\kappa s)ds. \quad (27)$$

In a manner similar to the accelerated current case the retarded current is normalized with respect to the random current of the retarded particles.

The steps involved in solving (27) follow the same general line as the integration of the first part of (12). The final result in the normalized form, $I_{rn}=I_r/I_d$, is given below:

$$I_{rn}=e^{V_0-\kappa^2}\sum_{n=0}^{\infty}\frac{(2n+1)!\kappa^n}{(n!)^2 2^{2n}(-V_0)^{n/2}}I_n[2\kappa(-V_0)^{\frac{1}{2}}], \quad (28)$$

where $V_0<0$ is to be taken.

If the electrons constitute the retarded current component then the series converges very rapidly since $\kappa \ll 1$. In that case for all practical purposes, κ may be set equal to zero and Eq. (28) reduces to

$$I_{rn}|_{\kappa=0}=e^{V_0}. \quad (29)$$

When the collector potential is negligibly small ($V_0 \cong 0$), then Eq. (28) in the limiting value as $V_0 \to 0$ becomes

$$I_{rn}|_{V_0=0}=e^{-\kappa^2}[(1+\kappa^2)I_0(\tfrac{1}{2}\kappa^2)+\kappa^2 I_1(\tfrac{1}{2}\kappa^2)]. \quad (30)$$

This represents the random current to the moving probe. For $\kappa=0$, which is true, in general, for electrons, Eq. (30) yields

$$I_{rn}|_{V_0=0,\kappa=0}=1. \quad (31)$$

In the above treatment of the retarded particles, one observes that a/r does not appear explicitly in the current functions. For this reason a second equation relating (a/r) and V_0 is not needed if density and temperature are to be determined from the probe characteristics. This is not the case for the accelerated particles where one needs a second independent relation for interpreting the above parameters.

III. DISCUSSION

Theory given so far is not specialized to the consideration of any particular kind of a particle. For instance, Eq. (19) for the normalized accelerated current is equally applicable to the positive and negative ions and electrons depending upon the polarity of the collector; the same holds for the retarded current relation given by Eq. (28). In practice, however, the probe characteristics are usually interpreted in the voltage range which is negative with respect to the plasma. Therefore, only the accelerated ion current and the retarded electron current characteristics are discussed here. In the accelerated ion current relation for finite a/r ratio given by Eq. (19), two parameters a/r and V_0 appear which are not independent of each other. For this reason one would need another independent relation between (a/r) and V_0 to eliminate one of the parameters from Eq. (19). Since no such independent relation exists for the moving probe which can be used profitably in that direction, the orbital-motion-limited mode of operation ($a/r \to \infty$) for the ion current is preferred. The retarded electron current, of course, is inherently independent of a/r.

The volt-ampere characteristics shown in Figs. 4–7 correspond to a typical experiment[6] in which a thin cylinder [0.023 in. (0.058 cm) in diameter and 7 in. (17.8 cm) long] is driven with respect to a reference sphere [8 in. (20.3 cm) in diameter]. In order to obtain these characteristic curves, it is important first to determine the equilibrium potential, also called the wall potential, of the reference sphere at the desired drift velocities of the system. Let V_{ws} denote the wall poten-

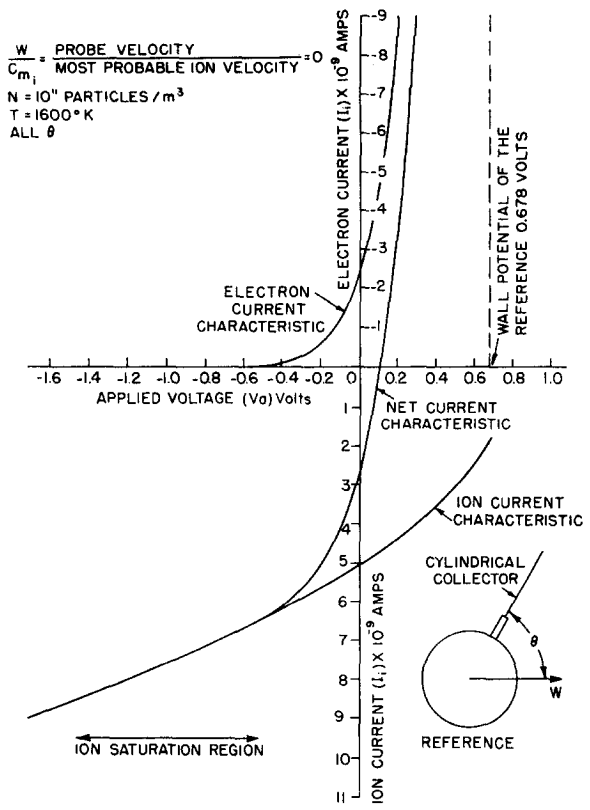

FIG. 4. A predicted volt–ampere characteristic of a thin cylindrical Langmuir probe, under typical F_1-region conditions, showing primarily the ion saturation region of the current characteristic.

tial of the sphere and V_{wc} that of the cylinder. The drift velocity of the vehicle tends to decrease $|V_{ws}|$ and $|V_{wc}|$ due to the increase in the collection of positive ions, whereas the electron collection is uneffected by such a motion. In the case of the cylinder V_{wc} is also orientation dependent. In plotting the volt–ampere characteristics, however, one needs only V_{ws} since the area ratio between the sphere and the cylinder is large enough to permit that. The technique used in plotting the characteristic curves is described below.

In an earlier report[4,6] the author has derived the volt–ampere relations for the moving spherical probes. The values of V_{ws} for various W/C_{m_i} may be obtained graphically by plotting the ion and the electron currents along the same axis and the voltage across the sheath along the other axis. Then the point where the two current components intersect yields the value of V_{ws} where the net current to the sphere is zero. Thus, for the typical values of the ionospheric parameters $N=10^{11}$ particles/m^3, $T=1600$°K and for the reasonable value of a/r (ratio of the sheath radius to the collector radius), say 1.1, it is found that $V_{ws}=-0.678$, -0.64, and -0.58 V, when $W/C_{m_i}=0$, 1, and 2, respectively. Having thus obtained the values of V_{ws} the volt–ampere characteristics of the cylinder may be obtained as follows.

First consider the case where the probe is stationary, $W=0$. Choosing a convenient horizontal scale representing the net voltage across the sheath of the cylinder, the orbital-motion-limited-ion current, Eq. (25), and the electron current, Eq. (29), are plotted as shown in Fig. 4. In this figure the scale for the net voltage is not shown; however, the point where the vertical dashed line is drawn represents the zero point on the original scale. To obtain the zero point for the scale which represents the applied voltage to the cylinder the vertical axis is shifted to the left by the amount equal to the wall potential of the reference, i.e., $|V_{ws}|=0.678$ V at $W/C_{m_i}=0$. The new origin then represents the zero applied voltage.

Figure 4 illustrates the stationary probe characteristics, $W=0$. The ion current component, Eq. (25), assuming atomic oxygen ions, is shown separately from the electron current component, Eq. (29). From this figure it is clear that when the applied voltage V_a is zero there is a net positive current to the probe which means that $|V_{wc}|<|V_{ws}|$. This can also be confirmed by computing V_{wc} by the same method as used in conjunction with the sphere. In fact, using Eqs. (25) and (29), it is found that $V_{wc}=-0.575$ V when $W=0$. Consequently, the net current to the probe is zero when a voltage of $+0.103$ V is applied to it with respect to the

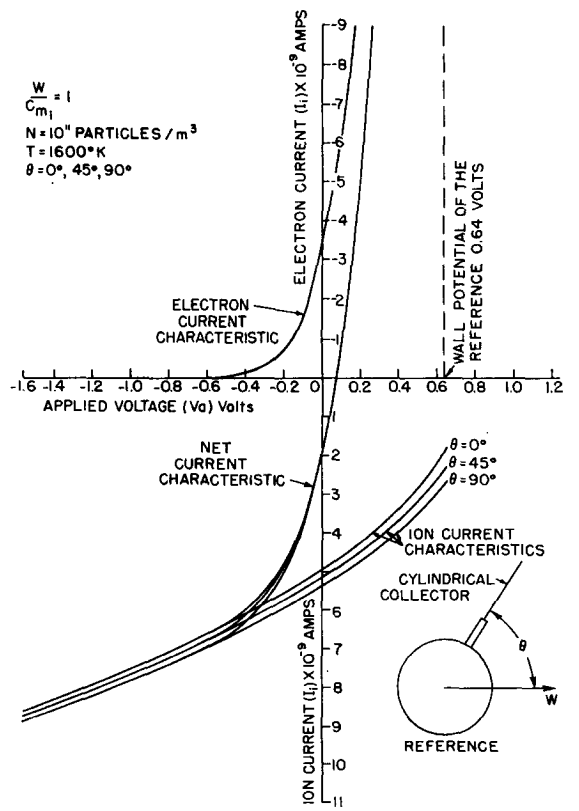

FIG. 5. A predicted volt–ampere characteristic of a cylindrical probe illustrating the effect of orientation upon the ion current characteristic at a fixed velocity ratio $W/C_{m_i}=1$.

reference. Figure 5 represents the volt-ampere characteristics for $W/C_{m_i}=1$ and range of θ as shown. Here the equation (24) containing W and θ was used for plotting the ion current components. As one would expect, the orientation is visible mostly in the positive ion current region. The wall potential of the reference is -0.64 V and that of the cylinder ranges from -0.565 to -0.54 V for $\theta=0°$ to 90°. Due to the decrease in $|V_{ws}|$, as a result of the probe motion, the net positive current at $V_a=0$ is smaller as compared to when $W=0$. Figure 6 demonstrates the similar behavior at $W/C_{m_i}=2$. Here the orientation effect is even more pronounced. It may be noted that in Figs. 4–6 the net current characteristics for $\theta=0$ are the same except for the corresponding shifts of the vertical axis depending upon the value of W/C_{m_i} as discussed.

In reducing the ion density from the experimental data, it is evident from Figs. 5 and 6 that the effects of orientation must be considered. Thus, knowing the magnitude of the measured current I_i, W, θ, V_{ws}, and the assumed value of the ion temperature and mass, one can determine the ion density from the following equation:

$$N_i=\frac{I_i}{(kT_i/2m_i\pi)^{\frac{1}{2}}eA_cI_{0n}}, \tag{32}$$

where I_{0n} is given by Eq. (24).

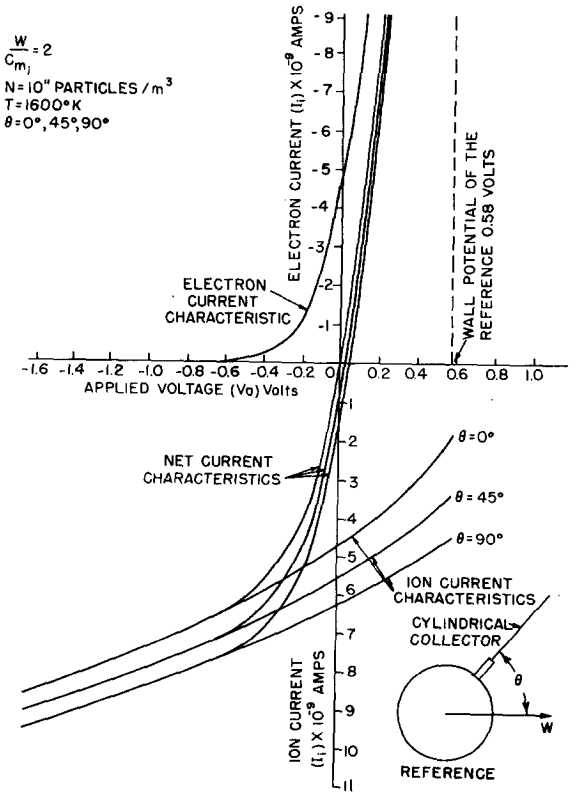

FIG. 6. A predicted volt-ampere characteristic of a cylindrical probe illustrating the effect of orientation upon the ion current characteristic at a fixed velocity ratio $W/C_{m_i}=2$.

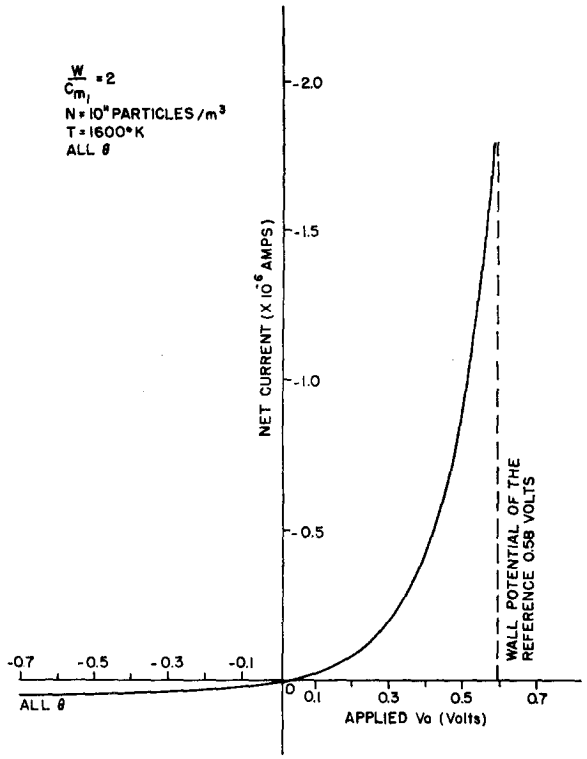

FIG. 7. A predicted volt-ampere characteristic of a cylindrical probe showing primarily the electron current region of the curve from which the electron temperature may be derived.

Since I_{0n} contains $V=V_{ws}+V_a$, where V is the net voltage across the sheath of the cylinder, one practical difficulty encountered in using the above equation is in determining V_{ws} from the experimental data. In fact no methods are available, which can be used with complete confidence, for obtaining this quantity from the data.

Finally, Fig. 7 illustrates the entire characteristics for $W/C_{m_i}=2$ and all θ. Since the ion current component for all θ is small compared with the electron current component, for V_a greater than a small positive value, the orientation angle has negligible effect on the electron temperature determination. Thus, with the help of Eq. (29), one can determine the electron temperature by the usual method of plotting the log of electron current vs the applied voltage.

ACKNOWLEDGMENTS

The author wishes to express his deep gratitude to George Carignan, Director of the Space Physics Research Laboratory of the University of Michigan, for reading the manuscript and making useful suggestions. He is especially grateful to Professor Andrew Nagy for many helpful discussions and suggestions. His thanks also extend to Dr. Ernest Fontheim for checking the theoretical section.

The work reported here was supported by the Goddard Space Flight Center of NASA under contract NASr-15.